Superdeformed multi-quasiparticle high-K states and possible isomers in Pb and Po isotopes

Yue Shi,[1] F.R. Xu,[1,*] P.M. Walker,[2,3] and G.D. Dracoulis[4]

[1]*State Key Laboratory of Nuclear Physics and Technology, School of Physics, Peking University, Beijing 100871, China*

[2]*Department of Physics, University of Surrey, Guildford, Surrey GU2 7XH, United Kingdom*

[3]*CERN, CH-1211 Geneva 23, Switzerland*

[4]*Department of Nuclear Physics, R.S.P.E., Australian National University, Canberra ACT 0200, Australia*

(Dated: May 27, 2012)

Abstract

Configuration-constrained potential-energy-surface calculations have been performed to investigate multi-quasiparticle high-K states built on superdeformed minima in ^{192,194,196}Pb, and ^{198}Po. The calculations predict that ^{196}Pb and ^{198}Po would be favorable candidates for the observation of low-lying superdeformed two- and four-quasiparticle high-K states. The possible decay paths and lifetimes that could lead to isomers are evaluated in detail for ^{196}Pb. Comparisons between the predictions and previous observations of octupole-vibrational excitations indicate also that bands built on superdeformed high-K intrinsic states may compete with the octupole-vibrational mode in this mass region. The quadrupole moments of both the collective and intrinsic excitations are analysed.

PACS numbers: 21.10.-k, 23.20.Lv, 27.80.+w

*Electronic address: frxu@pku.edu.cn

I. INTRODUCTION

Nuclei with extremely enlongated shapes have stimulated considerable interest among nuclear structure experimentalists and theorists for decades (see, e.g., Ref. [1] and references therein). Discrete γ-rays that characterize superdeformation have been observed in several mass regions of the nuclear chart, the $A \sim 150$ and 190 regions being the most well known. Since the first identification of the superdeformed (SD) band in ^{191}Hg [2], over 80 SD bands have been observed in 25 nuclei in the mass-190 region [1], constituting one of the most important data sets for the study of the superdeformation phenomenon.

Due to the difficulty in identifying linking transitions between SD and normally deformed (ND) bands presumably because of their low intensities and fragmented paths, the excitation energies, spin values, and parities of most SD bands are unknown. Intensity is generally transferred out of the bands before they reach the bandheads. Therefore the information concerning the structure of SD bands has been mainly obtained indirectly from the behaviour of the dynamic moment of inertia ($\mathscr{J}^{(2)}$) versus the rotational frequency [3, 4]. For even-even nuclei in the $A \sim 190$ region, the rise of $\mathscr{J}^{(2)}$ of yrast SD bands has been attributed to the gradual alignment of pairs of high-j intruder orbitals as predicted in various mean-field plus cranking calculations with explicit pairing [5–7]. In addition to the lowest SD bands, near-yrast excited SD bands also exhibit interesting features. For example, it has been suggested that the enhanced $E1$ transitions observed to link excited and yrast SD bands in ^{190,194}Hg [8, 9] and ^{196}Pb [10, 11] indicate octupole correlations in the SD minimum. This is supported by cranking plus random-phase-approximation (RPA) calculations which predict low excitation energies for octupole vibrational states in $^{190-194}$Hg [12], and by shell-correction calculations that indicate considerable octupole softness of the SD minima [13]. Furthermore, there must exist low-lying multi-quasiparticle (qp) states within the SD minima in this mass region, as commented on by Chasman [14].

The authors of Ref. [13] have performed extensive calculations for various one-qp states based on SD minima in odd-A Au ($Z = 79$), Tl ($Z = 81$), Bi ($Z = 83$), and Hg ($Z = 80$) isotopes. The results show a multitude of high-Ω configurations at low excitation energies some of which have been confirmed experimentally (see, e.g., Ref. [15]). Another feature of superdeformation in the $A \sim 190$ region which differentiates it from the $A \sim 150$ region is that the SD minimum appears already at zero frequency [13]. This fact together with the

occurrence of high-Ω orbits near the neutron and proton Fermi levels represents favourable conditions for the formation of high-K states. The possibility of the occurrence of SD high-K isomers in ^{196}Pb was discussed qualitatively in Ref. [16]. In Ref. [17], a few low-lying one- and two-qp SD bands were calculated using the cranked Hartree-Fock-Bogoliubov model. In the present work, we focus on SD, high-K, multi-qp, isomeric states. A systematic search for favorable states for the formation of SD high-K isomers has been performed, through the calculation of multi-qp high-K states in the superdeformed minima in even-even nuclei of this mass region. Comparisons of the present calculations with others that include various collective degrees of freedom, e.g., β-vibration, γ-vibration [18], or octupole-vibration [12], may provide the context for evaluating a competing mode, high-K intrinsic excitations and their associated collective rotation, which would be particularly interesting experimentally.

II. THE MODEL

We have used the macroscopic-microscopic model with the standard liquid-drop energy [19] and microscopic shell and pairing corrections. Single-particle levels which are needed in the calculation of the microscopic energy are given by the nonaxial deformed Woods-Saxon (WS) potential [20] with pairing correlations treated by the Lipkin-Nogami (LN) method [21]. The LN pairing avoids the spurious pairing phase transition encountered in the usual BCS approach. As in previous works [22, 23], the pairing strength (G) is determined initially by the average gap method [24] and then adjusted to reproduce the experimental odd-even mass differences using a five-point formula in both experiment and theory. The energy calculation of the macroscopic-microscopic model is standard as given, for example, in Ref. [25]. For a multi-qp state, however, the microscopic energy contains the contribution from the unpaired particles which occupy the single-particle orbits specified by the given configuration − see our previous work [23] for the detailed formulae. Blocking effects from the unpaired particles are taken into account by removing the orbitals making up the configuration from the LN pairing calculation.

In the macroscopic-microscopic model, the deformation of a state is obtained by minimizing the corresponding potential-energy-surface (PES). The configuration-constrained PES calculation [23] for a multi-qp state requires the adiabatic blocking of the configuration orbits in the considered deformation space (β_2, γ, β_4), i.e., the specific single-particle orbits are

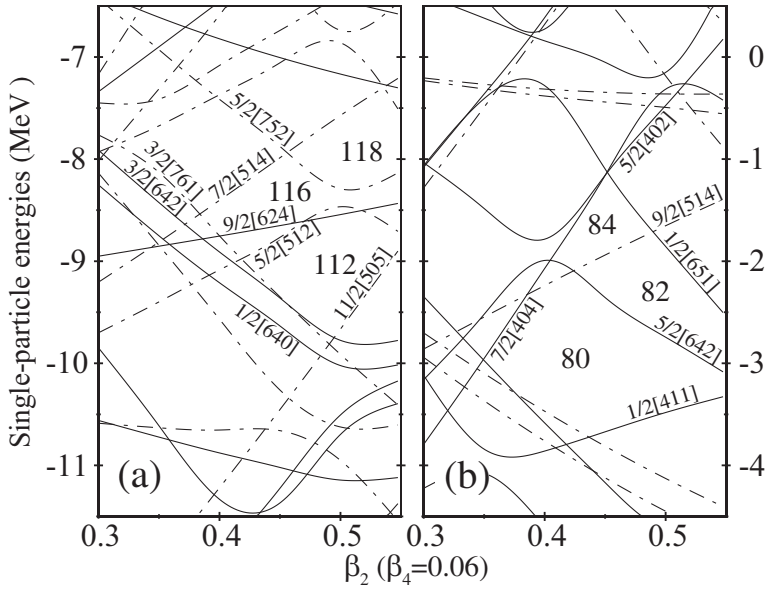

FIG. 1: Neutron (a) and proton (b) single-particle levels plotted against β_2-deformation ($\beta_4 = 0.06$, $\gamma = 0°$).

kept singly occupied while the deformation in the PES calculation is varied. This has been achieved by calculating and identifying the average Nilsson quantum numbers of every orbit involved in the configuration [23]. In the present model, the excitation energy which can be compared with experiment is obtained from the energy difference between the minima of the multi-qp and ground-state surfaces.

In order to see the relative energies between the multi-qp bandheads and the yrast SD states, we have performed pairing-deformation self-consistent total Routhian surface (TRS) calculations for the collective SD bands [21, 26]. Quadrupole pairing in doubly stretched coordinate space [27] has a negligible effect on energies, but it is included (with the strength determined by restoring the local Galilean invariance) because it has an important influence on collective angular momenta [28, 29].

III. CALCULATIONS AND DISCUSSIONS

A. High-K intrinsic states, configurations and deformations

Figure 1 shows the single-particle energies as a function of β_2 deformation, with β_4 and γ fixed at values that are typical for the SD minima in this mass region. The Nilsson diagrams

are very similar to those obtained in Ref. [13], for example. The shell gap responsible for superdeformation in the mass region is clearly visible at $\beta_2 \sim 0.46$ for $Z = 80$. However, the large shell gap results in relatively high energies for quasi-proton excitations. Since we are interested in low-lying high-K states, we confine our search to the even-even Pb and Po isotopes where SD bands have been observed, namely, ^{192,194,196}Pb and ^{198}Po. The high-Ω orbits mentioned in the introduction appear near the neutron and proton Fermi levels at $N = 114$ and $Z = 82$, respectively.

Figure 2 displays the calculated excitation energies as a function of spin for the yrast SD bands and various high-K multi-qp states in ^{192,194,196}Pb, and ^{198}Po. The detailed calculated results can be found in Tables I, II, III, and IV. Figure 2 also displays the experimental values for yrast SD bands in lead isotopes in which single-step transitions from SD bands to ND bands were observed [30–33]. For the yrast SD band of ^{192}Pb, the agreement between measurements and our calculations is very good. For ^{194,196}Pb, however, there is some disagreement between experiment and theory that is known to be related to the predicted positions of high-N intruder orbits [28, 29]. As has been noted, our main purpose in calculating the yrast SD bands is to see the relative energy difference between collective SD and multi-qp SD states.

While the lowest two-qp high-K states in ^{192,194}Pb are still about 1.5 MeV above their SD yrast line, the excitation energies of multi-qp states in $^{196}_{82}\mathrm{Pb}_{114}$ and $^{198}_{84}\mathrm{Po}_{114}$ relative to the second minima are in general lower (see Fig. 2). Among the calculated high-K states in ^{192,194,196}Pb and ^{198}Po, the two-quasineutron $\nu\{9/2^+[624], 5/2^-[512]\}, K^\pi = 7^-$ state in ^{196}Pb is predicted to have the lowest energy being 0.9 MeV higher than the yrast SD band. The 7^- configuration combined with the low-lying two-quasiproton $\pi\{9/2^-[514], 5/2^+[642]\}$ state leads to the lowest four-qp $K^\pi = 14^+$ state in ^{196}Pb. (The possibility of the formation of similar SD high-K isomers in this nucleus was commented on in Ref. [16].)

Some excited SD bands have been observed experimentally in the mass-190 region [1] but in most cases, the spins and excitation energies are unknown due to the absence of electromagnetic transitions connecting the excited SD bands to known states. In ^{190,194}Hg, and ^{196}Pb, enhanced $E1$ transitions between excited and yrast SD bands have been reported [9, 11, 34], although in general these bands have not been observed (presumably) down to their bandheads. The authors of Ref. [12] have performed cranked shell model (CSM) + RPA calculations for $^{190-194}$Hg. Their results suggest the prevalence of the octupole-

TABLE I: Calculated excitation energies E^* (relative to g.s. energy), energies with respect to SD minima (E^*_{SD}), β_2 and β_4 deformations, and quadrupole moments for various SD high-K states in ^{192}Pb. The calculated γ deformations are zero.

K^π	Configurations[a]		β_2	β_4	Q_{20}	E^*_{SD}	E^*
	Neutrons	Protons			(eb)	(keV)	(keV)
$0^+_{\rm sd}$	vacuum	vacuum	0.480	0.062	18.79	0	3996
7^+	$(\frac{11}{2}^-, \frac{3}{2}^-)$	vacuum	0.493	0.057	19.16	1601	5597
7^-_1	$(\frac{11}{2}^-, \frac{3}{2}^+)$	vacuum	0.494	0.067	19.19	1707	5703
4^-	$(\frac{5}{2}^-_x, \frac{3}{2}^+)$	vacuum	0.453	0.058	17.36	1732	5728
8^+_1	$(\frac{11}{2}^-, \frac{5}{2}^-_x)$	vacuum	0.484	0.057	18.80	1974	5970
6^+_1	$(\frac{9}{2}^+, \frac{3}{2}^+)$	vacuum	0.461	0.051	17.41	2032	6028
6^-	$(\frac{9}{2}^+, \frac{3}{2}^-)$	vacuum	0.471	0.053	18.33	2059	6055
10^-	$(\frac{11}{2}^-, \frac{9}{2}^+)$	vacuum	0.489	0.052	18.92	2153	6149
7^-_2	$(\frac{9}{2}^+, \frac{5}{2}^-_x)$	vacuum	0.442	0.047	16.85	2244	6240
8^+_2	$(\frac{11}{2}^-, \frac{5}{2}^-_y)$	vacuum	0.508	0.071	19.71	2479	6475
7^-_3	vacuum	$(\frac{9}{2}^-, \frac{5}{2}^+_x)$	0.466	0.051	18.06	1412	5408
6^+_2	vacuum	$(\frac{7}{2}^+, \frac{5}{2}^+_x)$	0.446	0.088	17.29	2176	6172
5^+	vacuum	$(\frac{5}{2}^+_x, \frac{5}{2}^+_y)$	0.453	0.065	17.62	2385	6381
11^+	$(\frac{5}{2}^-, \frac{3}{2}^+)$	$(\frac{9}{2}^-, \frac{5}{2}^+_x)$	0.452	0.053	17.21	3037	7033
14^-	$(\frac{11}{2}^-, \frac{3}{2}^-)$	$(\frac{9}{2}^-, \frac{5}{2}^+_x)$	0.485	0.051	18.52	3082	7078
14^+_1	$(\frac{11}{2}^-, \frac{3}{2}^+)$	$(\frac{9}{2}^-, \frac{5}{2}^+_x)$	0.485	0.054	18.61	3264	7260
13^-	$(\frac{9}{2}^+, \frac{3}{2}^+)$	$(\frac{9}{2}^-, \frac{5}{2}^+_x)$	0.456	0.048	17.24	3303	7299
13^+	$(\frac{9}{2}^+, \frac{3}{2}^-)$	$(\frac{9}{2}^-, \frac{5}{2}^+_x)$	0.463	0.049	17.99	3370	7366
14^+_2	$(\frac{9}{2}^+, \frac{5}{2}^-_x)$	$(\frac{9}{2}^-, \frac{5}{2}^+_x)$	0.444	0.046	16.85	3504	7500
17^+	$(\frac{11}{2}^-, \frac{9}{2}^+)$	$(\frac{9}{2}^-, \frac{5}{2}^+_x)$	0.479	0.051	18.42	3573	7569

[a] Neutrons: $\frac{5}{2}^-_x[512]$, $\frac{5}{2}^-_y[752]$ $\frac{3}{2}^+[642]$, $\frac{11}{2}^-[505]$, $\frac{9}{2}^+[624]$, $\frac{3}{2}^-[761]$; Protons: $\frac{9}{2}^-[514]$, $\frac{5}{2}^+_x[642]$, $\frac{5}{2}^+_y[402]$, $\frac{7}{2}^+[404]$.

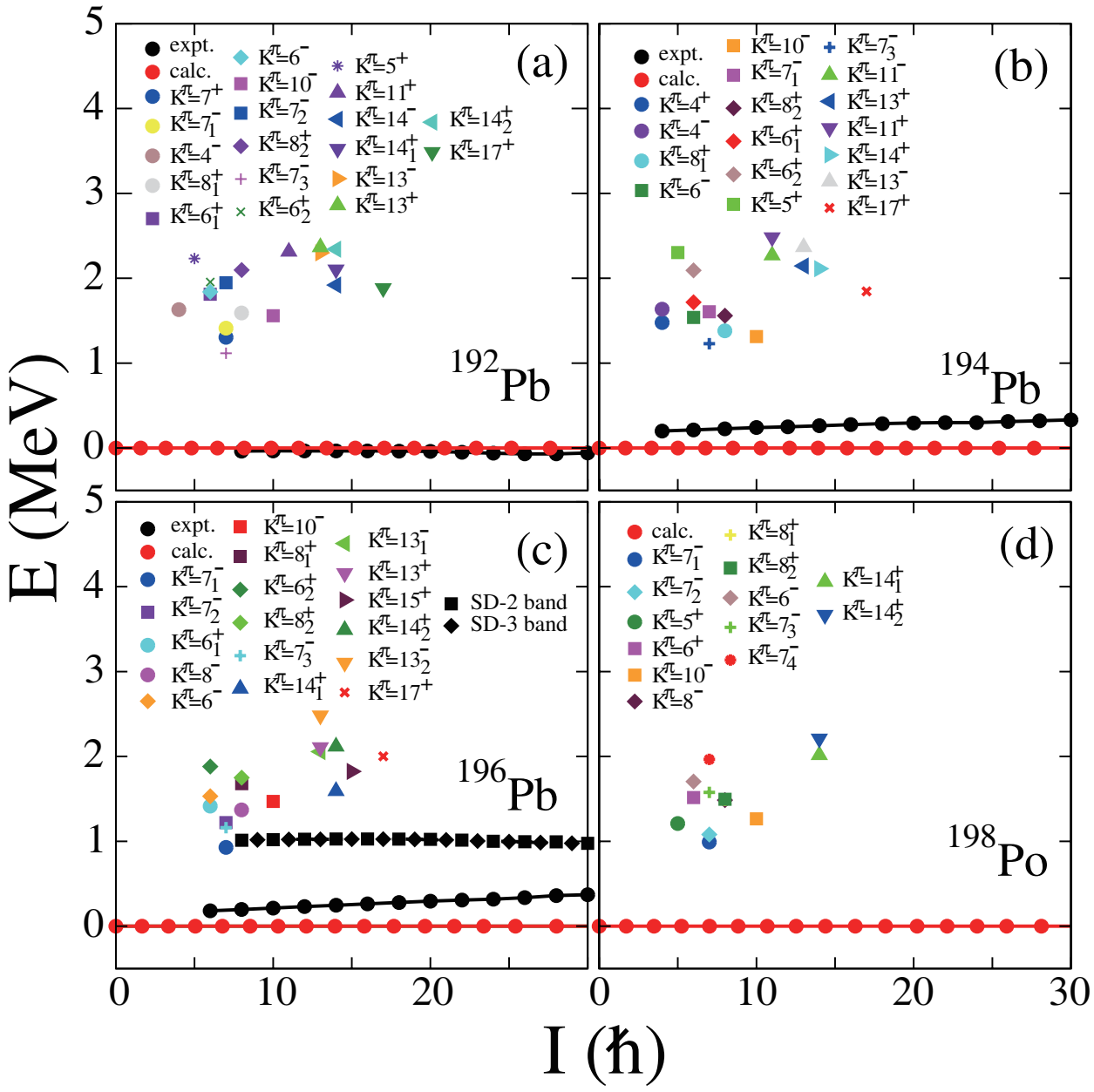

FIG. 2: (Color online). Excitation energies relative to the calculated yrast SD band. Experimental data are in black. A variety of multi-qp states are shown for ^{192}Pb [(a)], ^{194}Pb [(b)], ^{196}Pb [(c)], and ^{198}Po [(d)].

vibrational mode in low lying SD bands. The SD-2 and SD-3 bands in Fig. 2(c) for ^{196}Pb [11] have been proposed to be octupole-vibrational bands based on their calculations. Indeed, the low-K octupole character may explain the observed enhanced $E1$ transition.

The kinetic moment of inertia, $\mathscr{J}^{(1)}$, is an interesting observable which is sensitive to the intrinsic configuration. However, the configuration-constrained pairing-included Total-

TABLE II: Same as Table I, but for ^{194}Pb.

K^π	Configurations[a]		β_2	β_4	Q_{20}	E^*_{SD}	E^*
	Neutrons	Protons			(eb)	(keV)	(keV)
$0^+_{\rm sd}$	vacuum	vacuum	0.486	0.067	19.10	0	4476
4^+	$(\frac{5}{2}^-_x, \frac{3}{2}^-)$	vacuum	0.471	0.060	18.34	1576	6052
4^-	$(\frac{5}{2}^-_x, \frac{3}{2}^+)$	vacuum	0.472	0.066	18.67	1735	6211
8^+_1	$(\frac{11}{2}^-, \frac{5}{2}^-_x)$	vacuum	0.499	0.064	19.40	1744	6220
6^-	$(\frac{9}{2}^+, \frac{3}{2}^-)$	vacuum	0.474	0.055	18.44	1749	6225
10^-	$(\frac{11}{2}^-, \frac{9}{2}^+)$	vacuum	0.502	0.059	19.43	1877	6353
7^-_1	$(\frac{9}{2}^+, \frac{5}{2}^-_x)$	vacuum	0.468	0.054	18.23	1886	6362
8^+_2	$(\frac{11}{2}^-, \frac{5}{2}^-_y)$	vacuum	0.508	0.076	19.74	1924	6400
6^+_1	$(\frac{9}{2}^+, \frac{3}{2}^+)$	vacuum	0.474	0.062	18.62	1928	6404
6^+_2	$(\frac{7}{2}^-, \frac{5}{2}^-_x)$	vacuum	0.456	0.053	17.38	2303	6779
5^+	$(\frac{5}{2}^-_x, \frac{5}{2}^-_y)$	vacuum	0.491	0.063	19.23	2448	6924
7^-_3	vacuum	$(\frac{9}{2}^-, \frac{5}{2}^+)$	0.475	0.055	18.26	1509	5985
11^-	$(\frac{5}{2}^-_x, \frac{3}{2}^-)$	$(\frac{9}{2}^-, \frac{5}{2}^+)$	0.466	0.053	18.02	2955	7431
13^+	$(\frac{9}{2}^+, \frac{3}{2}^-)$	$(\frac{9}{2}^-, \frac{5}{2}^+)$	0.469	0.050	18.18	3099	7575
11^+	$(\frac{5}{2}^-_x, \frac{3}{2}^+)$	$(\frac{9}{2}^-, \frac{5}{2}^+)$	0.465	0.058	18.09	3167	7643
14^+	$(\frac{9}{2}^+, \frac{5}{2}^-_x)$	$(\frac{9}{2}^-, \frac{5}{2}^+)$	0.464	0.050	18.05	3211	7687
13^-	$(\frac{9}{2}^+, \frac{3}{2}^+)$	$(\frac{9}{2}^-, \frac{5}{2}^+)$	0.467	0.052	18.09	3321	7797
17^+	$(\frac{11}{2}^-, \frac{9}{2}^+)$	$(\frac{9}{2}^-, \frac{5}{2}^+)$	0.491	0.053	18.85	3450	7926

[a] Neutrons: $\frac{5}{2}^-_x[512]$, $\frac{5}{2}^-_y[752]$, $\frac{3}{2}^+[642]$, $\frac{11}{2}^-[505]$, $\frac{9}{2}^+[624]$, $\frac{3}{2}^-[761]$, $\frac{7}{2}^-[514]$; Protons: $\frac{9}{2}^-[514]$, $\frac{5}{2}^+[642]$.

Routhian-Surface (TRS) method has not been always successful for the calculation of rotational bands associated with multi-qp configurations, due to a convergence problem of our code. But in the case of the lowest-energy state of a given seniority, the configuration-constrained TRS calculation do converge successfully. We have attempted such TRS calculations for the collective rotation of the 2 quasi-proton, 2 quasi-neutron $K^\pi = 14^+$ states. The 14^+_2 state has higher energy than that of the 14^+_1 state but the associated rotational band falls quickly with increasing rotational frequency due to the presence of the high-j

TABLE III: Same as Table I, but for ^{196}Pb.

K^π	Configurations[a]		β_2	β_4	Q_0	E^*_{SD}	E^*
	Neutrons	Protons			(eb)	(keV)	(keV)
$0^+_{\rm sd}$	vacuum	vacuum	0.483	0.061	18.83	0	5520
7^-_1	$(\frac{9}{2}^+, \frac{5}{2}^-_x)$	vacuum	0.482	0.063	18.89	1189	6709
7^-_2	$(\frac{9}{2}^+, \frac{5}{2}^-_y)$	vacuum	0.499	0.072	19.46	1483	7003
6^+_1	$(\frac{7}{2}^-, \frac{5}{2}^-_x)$	vacuum	0.473	0.058	18.40	1607	7127
8^-	$(\frac{9}{2}^+, \frac{7}{2}^-)$	vacuum	0.474	0.052	18.42	1718	7238
6^-	$(\frac{9}{2}^+, \frac{3}{2}^-)$	vacuum	0.468	0.049	18.21	1722	7242
10^-	$(\frac{11}{2}^-, \frac{9}{2}^+)$	vacuum	0.503	0.054	19.44	2016	7536
8^+_1	$(\frac{11}{2}^-, \frac{5}{2}^-_x)$	vacuum	0.504	0.054	19.46	2026	7546
6^+_2	$(\frac{9}{2}^+, \frac{3}{2}^+)$	vacuum	0.472	0.054	18.39	2072	7592
8^+_2	$(\frac{11}{2}^-, \frac{5}{2}^-_y)$	vacuum	0.509	0.057	19.64	2096	7616
7^-_3	vacuum	$(\frac{9}{2}^-, \frac{5}{2}^+)$	0.476	0.050	18.31	1423	6943
14^+_1	$(\frac{9}{2}^+, \frac{5}{2}^-_x)$	$(\frac{9}{2}^-, \frac{5}{2}^+)$	0.475	0.054	18.33	2668	8188
13^-_1	$(\frac{5}{2}^-_x, \frac{7}{2}^-)$	$(\frac{9}{2}^-, \frac{5}{2}^+)$	0.468	0.050	18.18	2986	8506
13^+	$(\frac{9}{2}^+, \frac{3}{2}^-)$	$(\frac{9}{2}^-, \frac{5}{2}^+)$	0.463	0.049	18.03	3037	8557
15^+	$(\frac{9}{2}^+, \frac{7}{2}^-)$	$(\frac{9}{2}^-, \frac{5}{2}^+)$	0.467	0.049	18.09	3060	8580
14^+_2	$(\frac{9}{2}^+, \frac{5}{2}^-_y)$	$(\frac{9}{2}^-, \frac{5}{2}^+)$	0.487	0.054	18.80	3192	8712
13^-_2	$(\frac{9}{2}^+, \frac{3}{2}^+)$	$(\frac{9}{2}^-, \frac{5}{2}^+)$	0.465	0.049	18.06	3411	8931
17^+	$(\frac{11}{2}^-, \frac{9}{2}^+)$	$(\frac{9}{2}^-, \frac{5}{2}^+)$	0.490	0.053	18.84	3587	9107

[a] Neutrons: $\frac{5}{2}^-_x[512]$, $\frac{5}{2}^-_y[752]$, $\frac{3}{2}^+[642]$, $\frac{11}{2}^-[505]$, $\frac{9}{2}^+[624]$, $\frac{3}{2}^-[761]$, $\frac{7}{2}^-[514]$; Protons: $\frac{9}{2}^-[514]$, $\frac{5}{2}^+[642]$.

low-Ω intruder orbital ($\nu 5/2^-[752]$), and becomes lower energetically than the 14^+_1 band at $\hbar\omega > 0.15$ MeV. (See section III B for related discussions.) Figure 3 shows $\mathscr{J}^{(1)}$ for the predicted lowest-energy 4-qp $K^\pi = 14^+_2$ state (see table III) in ^{196}Pb as a function of rotation frequency. It is seen that $\mathscr{J}^{(1)}$ in the 14^+_2 SD band is significantly larger than that in the yrast SD band, which would indicate the reduced superconductivity in the pairing-blocked high-K state and also the contributions (essentially alignments) from the rotational motions of the unpaired component particles (see, for example Ref. [35]).

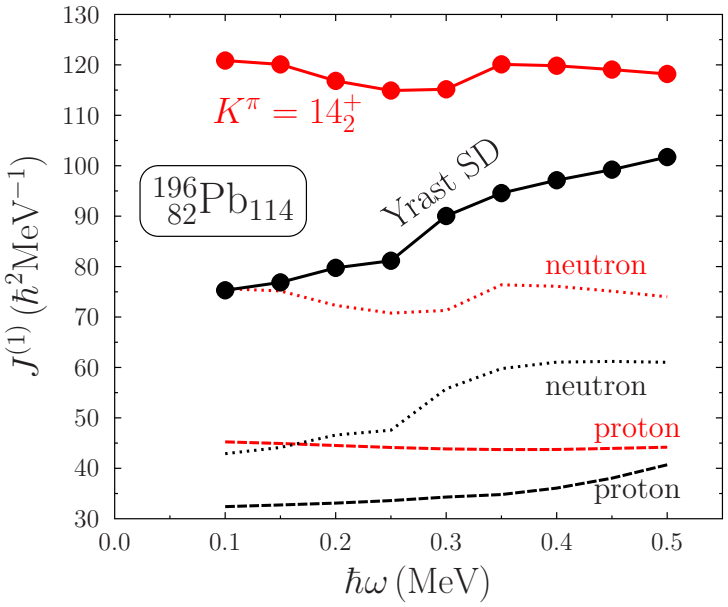

FIG. 3: (Color online). Calculated kinematic moment of inertia for the $K^\pi = 14_2^+$ (see Table III) high-K SD band in ^{196}Pb. The high-K results are in red, and the yrast SD results in black.

For a multi-qp state, the quadrupole moment is another important observable that provides information on the deformation and configuration. In the present model, the intrinsic quadrupole moment is calculated by $Q_{20} = \sum q_{k_j} + \sum_{k\neq k_j} 2V_k^2 q_k$, where q_k is the single-particle quadrupole moment of the k-th orbit given in the WS model. The first term gives the contribution from the unpaired particles that stay on the k_j-th orbit, and the second term is from all the paired particles that occupy the WS orbits with probabilities V_k^2 in the LN pairing model. Blocking effects are taken into account by restricting $k \neq k_j$ in the sum. The quadrupole moment thus calculated is configuration-dependent. In Tables I, II, III, and IV, we tabulate the quadrupole moments for multi-qp and ground states.

Experimentally, transition quadrupole moments for the yrast SD bands of some mercury and lead isotopes have been deduced from lifetime measurements. The latest data for even-even $^{192-196}$Pb, $19.6^{+0.5}_{-0.4}$ eb [36], $20.1^{+0.3}_{-0.5}$ eb [37], and $19.7^{+0.3}_{-0.3}$ eb [38], respectively, are well reproduced by the present calculations of 18.79 eb, 19.01 eb, and 18.83 eb, respectively. (One should notice that an extra systematic error ($\sim 15\%$) should be added to the measured values due to the uncertainty associated with the stopping power [36].) Of particular interest is that in Ref. [38] the lifetimes of both the yrast and one excited SD band [SD-2 band in Fig. 2(c)] have been observed. The deduced quadrupole moments of these two bands have

TABLE IV: Same as Table IV, but for ^{198}Po.

K^π	Configurations[a]		β_2	β_4	Q_{20}	E^*_{SD}	E^*
	Neutrons	Protons			(eb)	(keV)	(keV)
$0^+_{\rm sd}$	vacuum	vacuum	0.501	0.058	19.49	0	3729
7^-_1	$(\frac{9}{2}^+, \frac{5}{2}^-_x)$	vacuum	0.488	0.067	19.10	1258	4987
7^-_2	$(\frac{9}{2}^+, \frac{5}{2}^-_y)$	vacuum	0.508	0.078	20.08	1348	5077
5^+	$(\frac{5}{2}^-_x, \frac{5}{2}^-_y)$	vacuum	0.504	0.077	19.82	1349	5078
6^+	$(\frac{7}{2}^-, \frac{5}{2}^-_x)$	vacuum	0.478	0.061	18.87	1716	5445
10^-	$(\frac{11}{2}^-, \frac{9}{2}^+)$	vacuum	0.527	0.070	21.15	1813	5542
8^+_1	$(\frac{11}{2}^-, \frac{5}{2}^-_x)$	vacuum	0.521	0.067	20.82	1835	5564
8^-	$(\frac{9}{2}^+, \frac{7}{2}^-)$	vacuum	0.480	0.057	18.90	1840	5569
8^+_2	$(\frac{11}{2}^-, \frac{5}{2}^-_y)$	vacuum	0.527	0.067	21.06	1850	5579
6^-	$(\frac{9}{2}^+, \frac{3}{2}^-)$	vacuum	0.467	0.050	18.34	1905	5634
7^-_3	vacuum	$(\frac{9}{2}^-, \frac{5}{2}^+_x)$	0.493	0.068	18.94	1844	5573
7^-_4	vacuum	$(\frac{9}{2}^-, \frac{5}{2}^+_y)$	0.463	0.057	18.32	2233	5962
14^+_1	$(\frac{9}{2}^+, \frac{5}{2}^-_x)$	$(\frac{9}{2}^-, \frac{5}{2}^+_x)$	0.485	0.067	18.78	3081	6810
14^+_2	$(\frac{9}{2}^+, \frac{5}{2}^-_y)$	$(\frac{9}{2}^-, \frac{5}{2}^+_x)$	0.503	0.073	19.72	3274	7003

[a] Neutrons: $\frac{5}{2}^-_x[512]$, $\frac{5}{2}^-_y[752]$, $\frac{3}{2}^+[642]$, $\frac{11}{2}^-[505]$, $\frac{9}{2}^+[624]$, $\frac{3}{2}^-[761]$, $\frac{7}{2}^-[514]$; Protons: $\frac{9}{2}^-[514]$, $\frac{5}{2}^+_x[642]$, $\frac{5}{2}^+_y[402]$.

similar values, and the authors of Ref. [38] took this as evidence for octupole-vibrational character of SD-2 and SD-3 bands, because it was expected that the different occupations of configuration orbits should lead to different deformations [38]. However, our calculations give only a small shape-polarization effect of the $\nu 9/2^+[624]$ and $\nu 5/2^-[512]$ orbits and the resulting quadrupole moment of the $K^\pi = 7^-$ state is almost the same as that of the vacuum SD state (see Table. III).

B. Evaluation of high-K rotational bands and isomeric decays in ^{196}Pb

While the results above show that there will be high-K states that fall not far from the yrast line, the question remains as to what extent such states will be both populated and result in isomers. As a step towards addressing this question, the associated rotational bands have been calculated for the case of ^{196}Pb, using the VMI formulation incorporating a configuration-dependent alignment, and beginning with moments-of-inertia obtained from fits with the Harris formula to the $K = 0$ (yrast) SD-band. The contributions of different components in the configuration are included using the approach discussed in Ref. [35]. Alignments for each orbital were calculated using the cranked shell model (CSM) and combined assuming additivity. As discussed in Ref. [35], such a sum should be seen as the maximum alignment, since blocking will reduce the pairing, and thus the alignment, although this is likely to be a small effect in the present cases of very large deformation.

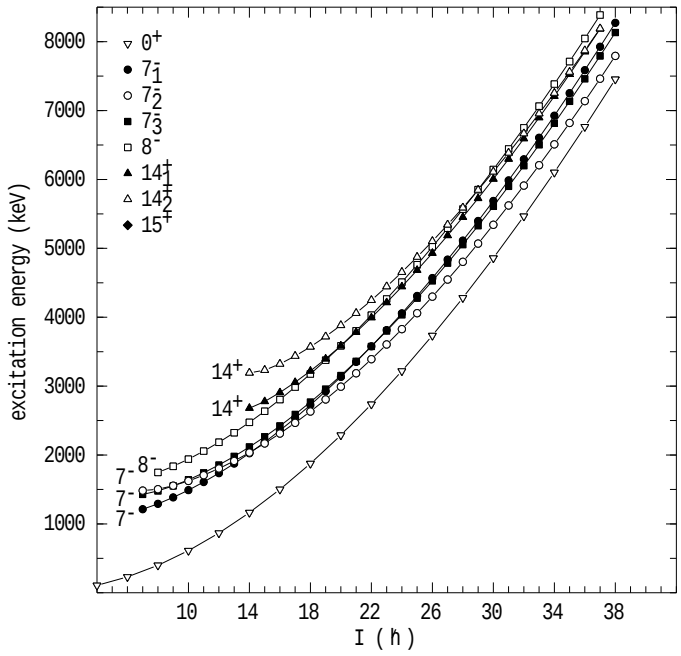

FIG. 4: Calculated high-K rotational bands relative to the $K = 0$ SD-band as a function of angular momentum for ^{196}Pb.

The key orbitals to contribute will be those of high-j parentage, specifically the $9/2^+[624]$ ($i_{13/2}$) neutron, the $5/2^-[752]$ ($j_{15/2}$) neutron and the $5/2^+[642]$ ($i_{13/2}$) proton. The configuration labeled 7^-_2 contains two of these orbitals, while the 14^+_2 configuration contains all three.

The calculated bands are depicted in Fig. 4 together with the $K^\pi = 0^+$, SD-band. (Note however that the latter is from a fit to the yrast band, not the experimental values.) Without alignment, the trajectories of each of the high-K bands would be approximately parallel to the yrast band. With an alignment contribution, several of the bands, particularly those from the 7_2^- and 14_2^+ configurations (as labeled in Table III), gain significantly, and approach the yrast region near spins of $30\hbar$. Some of these states are close to, and even lower in energy than, members of the octupole SD bands [39], so they are bound to receive significant population.

Once populated, the high K-hindrance will help to confine the decay path to be within the band, maintaining the population down to the band-heads, more so than is the case in the $K = 0$ and octupole SD-bands where the population transfers out to the normally-deformed (ND) states below about $7\hbar$. This leads to the second part of the question proposed earlier. That is, to what extent will this result in bandheads with significant lifetimes? This question cannot be answered precisely since small changes in energy cause large changes for high multipolarity transitions and the presence of small K-admixtures in states connected by otherwise forbidden transitions can strongly affect lifetimes. Furthermore, hindrances for a given forbiddenness can vary widely. Nevertheless, an order-of-magnitude guide can be formulated.

The quantities of interest are the transition strengths in terms of the Weisskopf estimates, or more conveniently, its inverse, $F = \tau_\gamma/\tau_W$, and the shortfall in the difference in K compared to the transition multipolarity (λ), termed the forbiddenness $\nu = \Delta K - \lambda$. The so-called "reduced hindrance", given by $f_\nu = F^{1/\nu}$ normally falls in the range 30-300, but for the present purposes we can adopt $f_\nu = 100$ for all cases.

A possible decay scheme constructed from the calculated high-K bands in ^{196}Pb is presented in Fig. 5. Selected transitions are listed in Table V. The scheme and table do not include all possible decays but rather, those that are useful in highlighting the likely issues. As well as the hindrances (F) which scale according to the above assumptions as 100^ν, intrinsic decay strengths are required: the transitions involved are not collective and for simplicity we have assumed that "normal" strengths (those not involving K-hindrance) are specifically 0.1 W.u. for $M1$ transitions, 10^{-4} W.u. for $E1$ transitions and 1 W.u. for both $E2$ and $E3$ transitions. (Realistically, these are probably over-estimates of the strengths, depending on the configuration changes, so that the lifetimes could be under-estimates.)

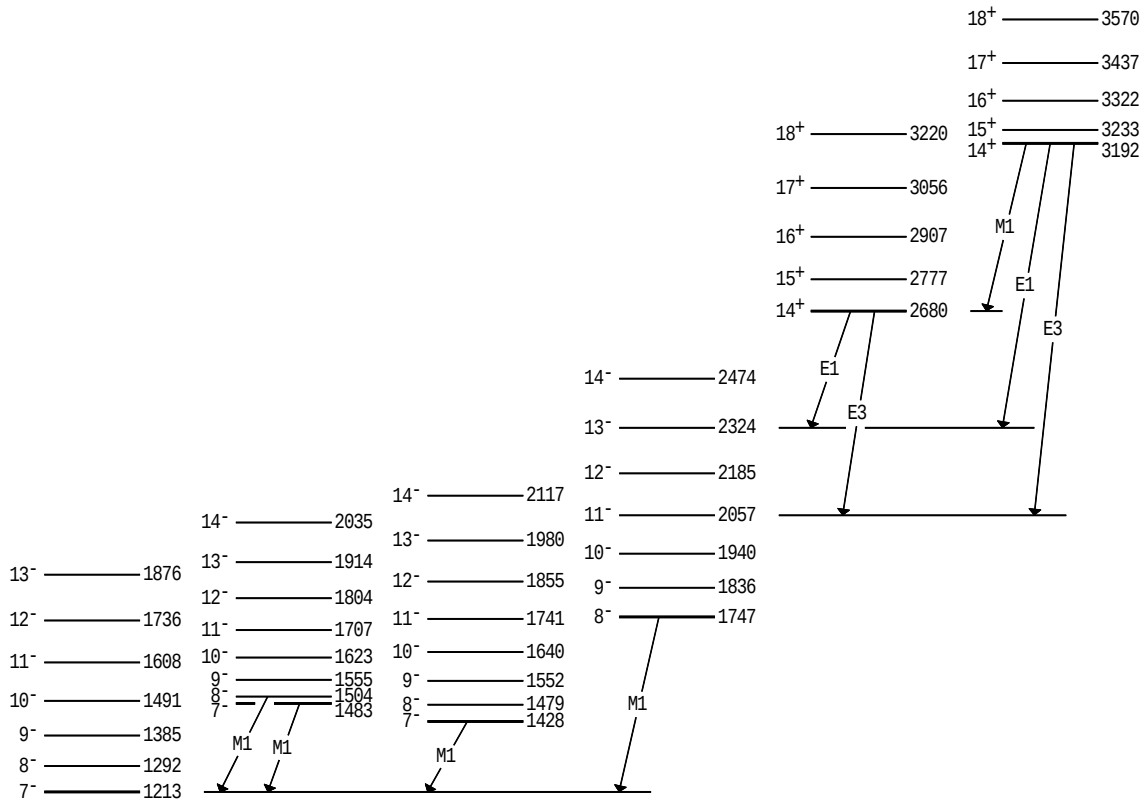

FIG. 5: Notional decay scheme of calculated high-K SD-bands in ^{196}Pb, showing the main decay paths expected between bands. Energies are in keV, relative to the SD minimum.

The final column in Table V gives the partial γ-ray lifetimes. (Final lifetimes would require combination of all branches and inclusion of internal conversion.)

Consider now, the decay proceeding from initial population of the highest intrinsic state at 3192 keV in the figure, arising from the 14_2^+ configuration. Given the short lifetime of the allowed 512-keV, $M1$ decay, the $E1$ and $E3$ branches would not compete hence the population would transfer, in a short time, to the 14_1^+ state. That state, however, does not have an equivalent fast decay path, so its lifetime will be controlled by its $E1$ and $E3$ decays, predominantly the 356-keV $E1$ to the 13^- member of the 8^- band, whose partial lifetime is predicted to be long, in the region of 600 ms. (Other paths to the lower octupole band and $K = 0$ SD-bands do not compete despite the much higher energies because the additional K-hindrances override the gain from the energy factors.)

In contrast, as can be seen from Table V, not one of the 8^-, 7_3^- and 7_2^- states is likely to have a lifetime in excess of a few nanoseconds, since all have allowed $M1$ decay paths. This leads us to the possibilities for the decays of the lowest of the intrinsic states, the 7_1^- state

TABLE V: Selected decays for calculated high-K SD-bands in ^{196}Pb expressed as partial γ-ray meanlives.

E_γ [a]	$\sigma\lambda$	E_f [b]	J^π; K^π	class.	ν	F [c]	τ_γ
3192 keV; $K^\pi = 14^+$							
512	M1	2680	14^+;14^+	SD-SD	(0)	10	0.2 ns
868	E1	2324	13^-; 8^-	SD-SD	5	$10^{10}\times10^4$	44 ms
1135	E3	2057	11^-; 8^-	SD-SD	3	10^6	315 ms
2680 keV; $K^\pi = 14^+$							
356	E1	2324	13^-; 8^-	SD-SD	5	$10^{10}\times10^4$	640 ms
623	E3	2057	11^-; 8^-	SD-SD	3	10^6	21 s
1747 keV; $K^\pi = 8^-$							
534	M1	1213	7^-; 7^-	SD-SD	(0)	10	0.21 ns
1428 keV; $K^\pi = 7^-$							
215	M1	1213	7^-; 7^-	SD-SD	(0)	10	3.2 ns
1483 keV; $K^\pi = 7^-$							
291	M1	1213	7^-; 7^-	SD-SD	(0)	10	1.3 ns
270	M1	1213	7^-; 7^-	SD-SD	(0)	10	1.6 ns
1213 keV; $K^\pi = 7^-$							
263	M1	950	6^-; 3^-	SD-SD	3	$10^6\times10$	17 μs
5274	E2	1798[d]	5^-; (0)	SD-ND	5	10^{10}	30 μs

[a]The bandhead energies differ slightly from the raw 2-qp energies in Table III because of rotational contributions.

[b]Energies are in keV, relative to the SD minimum, unless otherwise indicated.

[c]Hindrance factors of 10 for $M1$ and 10^4 for $E1$ assumed (see text).

[d]Absolute excitation energy. See Wilson *et al.* for measured excitation energy of the SD states [33].

calculated to lie at 1213 keV in the SD well. Several decays are possible but the two shown in Table V are considered the most relevant: an $M1$ decay to the 6^- state of the octupole SD-band and a possible $E2$ decay of high energy (5.274 MeV) to the 5^- state at 1798 keV in the ND well. Although the octupole SD-band is only observed down to its 8^- member, the energy of the 6^- state can be estimated by extrapolation. In the case of the $E2$ decay, the

K-value of the final 5^- state is not defined since it arises from a spherical configuration. As well as this uncertainty which might affect the calculation of the hindrance, there may be an additional hindrance due to the change in shape. Notwithstanding these qualifications, both decay branches are predicted to be slow and of comparable magnitude, leading to the expectation of an isomer with a mean-life in the region of microseconds or more.

To be consistent, there should be another qualification in the discussion above that relates to the alignment. Alignment is a manifestation of Coriolis mixing and therefore additional K-components will be present in the wave-function, although these are probably less significant in the case of the 7_1 and 14_1 states that turn out to be of most interest in terms of isomers. A further consideration that is of interest is the prospect for probing general (random) mixing in regions of high level density that result in the dilution of the K-quantum number [40, 41]. The isomers here are predicted to have lifetimes long enough that even with significant mixing, the resultant lifetimes could still be amenable to the techniques of time correlations. They could therefore remain as a useful (direct) probe of such effects, an opportunity that was also recognized by Åberg [16].

C. Octupole band character and the 7_1^- band

The calculations presented earlier predict the lowest $K^\pi = 7_1^-$ at 1189 keV in the SD well, not far above the odd-spin signature sequence of the observed SD band currently attributed to octupole vibrations [11]. As is common, intensity is transferred out of that band (presumably)before its (unknown) lowest states are reached, but extrapolation down from the observed 9^- member would place its 7^- state at about 900 keV. This is close enough to our predicted high-K state that it is appropriate to consider whether the structures could in fact be the same bands. There are several experimental properties that argue against this but possibly the most compelling is the absence of the expected cascade transitions between the odd- and even-spin signature partners in the case of high-K bands, as argued qualitatively in Ref. [11]. The intensity ratio of the crossover ($\Delta J = 2$) to cascade ($\Delta J = 1$) γ-ray transitions (λ_γ) depends on the value of $(g_K - g_R)/Q_0$ which depends on the configuration. For SD bands the quadrupole moment is large (~ 19 eb for these cases) thus generally favoring the $\Delta J = 2$ transitions, but for the 7_2^- configuration, $(g_K - g_R)$, will be about -0.73 (assuming $g_R = +0.4$) so that cascade transitions are expected to compete. For example the predicted

γ-ray branching ratios are $\lambda_\gamma = 1.8$, 1.6, 1.3 for the 17^-, 16^- and 15^- states of the $K = 7^-$ band. The cascade γ-ray transitions progress to become equal to, or even more intense than, the crossover transitions at lower spins. Although of lower energy, such transitions should have been within the sensitivity of previous measurements. Note that at even lower spins the cascade transitions will dominate, particularly when internal conversion is included. Note also, that the measured out-of-band $E1$ transitions observed from the octupole SD band have a strength of $\sim 10^{-4}$ W.u. [11], which are considered to be large, consistent with their special octupole character, underlining the conservative nature of our estimates ($F = 10^4$) in the analysis of competing $E1$ decays from the high-K bands.

IV. SUMMARY

We have performed configuration-constrained PES calculations for multi-qp high-K states based on SD minima in ^{192,194,196}Pb, and ^{198}Po. Some of the calculated high-K states show low energies relative to the yrast SD states. For ^{196}Pb and ^{198}Po, in particular two- and four-quasiparticle states are predicted to be located only ~ 1 MeV above the SD yrast line. From specific evaluations for ^{196}Pb it is shown that because of the presence of high-j components in the multi-particle configurations, rotational bands based on these configurations could compete for intensity at the higher spins and thus be populated with significant intensities. In several cases, the bandhead decays are predicted to be strongly inhibited, leading to isomers. These could provide an additional experimental sensitivity and also be used as probes of K-mixing in regions of high level density.

V. ACKNOWLEDGMENTS

This work has been supported by the Natural Science Foundation of China under Grant No. 10975006, the UK STFC, and AWE plc and the Australian Research Council discovery program.

---

[1] B. Singh, R. Zywina, and R. B. Firestone, Nucl. Data Sheet **97**, 241 (2002).

[2] E. F. Moore, R. V. F. Janssens, R. R. Chasman, I. Ahmad, T. L. Khoo, F. L. H. Wolfs, D. Ye, K. B. Beard, U. Garg, M. W. Drigert, et al., Phys. Rev. Lett. **63**, 360 (1989).

[3] T. Bengtsson, I. Ragnarsson, and S. Aberg, Phys. Lett. **B208**, 39 (1988).

[4] W. Nazarewicz, R. Wyss, and A. Johnson, Nucl. Phys. **A503**, 285 (1989).

[5] M. A. Riley, D. M. Cullen, A. Alderson, I. Ali, P. Fallon, P. D. Forsyth, F. Hanna, S. M. Mullins, J. W. Roberts, J. F. Sharpey-Schafer, et al., Nucl. Phys. **A512**, 178 (1990).

[6] B. Gall, P. Bonche, J. Dobaczewski, H. Flocard, and P.-H. Heenen, Z. Phys. A **348**, 183 (1994).

[7] A. V. Afanasjev, P. Ring, and J. König, Nucl. Phys. **A676**, 196 (2000).

[8] B. Crowell, M. P. Carpenter, R. V. F. Janssens, D. J. Blumenthal, J. Timar, A. N. Wilson, J. F. Sharpey-Schafer, T. Nakatsukasa, I. Ahmad, A. Astier, et al., Phys. Rev. C **51**, 1599(R) (1995).

[9] G. Hackman, T. L. Khoo, M. P. Carpenter, T. Lauritsen, A. Lopez-Martens, I. J. Calderin, R. V. F. Janssens, D. Ackermann, I. Ahmad, S. Agarwala, et al., Phys. Rev. Lett. **79**, 4100 (1997).

[10] S. Bouneau, F. Azaiez, J. Duprat, I. Deloncle, M.-G. Porquet, U. J. van Severen, T. Nakatsukasa, M.-M. Aléonard, A. Astier, G. Baldsiefen, et al., Z. Phys. A **358**, 179 (1997).

[11] D. Roßbach, A. Görgen, H. Hübel, E. Mergel, G. Schönwaßer, A. N. Wilson, F. Azaiez, A. Astier, D. Bazzacco, M. Bergström, et al., Phys. Lett. **B513**, 9 (2001).

[12] T. Nakatsukasa, K. Matsuyanagi, S. Mizutori, and Y. R. Shimizu, Phys. Rev. C **53**, 2213 (1996).

[13] W. Satuła, S. Ćwiok, and W. Nazarewicz, Nucl. Phys. **A529**, 289 (1991).

[14] R. R. Chasman, Phys. Rev. Lett. **80**, 4610 (1998).

[15] M. J. Joyce, J. F. Sharpey-Schafer, P. J. Twin, C. W. Beausang, D. M. Cullen, M. A. Riley, R. M. Clark, P. J. Dagnall, I. Deloncle, J. Duprat, et al., Phys. Rev. Lett. **71**, 2176 (1993).

[16] S. Åberg, in *Proceedings of the La Rabida summer school*, edited by J. M. Arias, M. I. Gallardo, and M. Lozano (Springer-Verlag, Heulva, Spain, 1994), pp. 211–229.

[17] P.-H. Heenen and R. V. F. Janssens, Phys. Rev. C **57**, 159 (1998).

[18] J. Libert, M. Girod, and J.-P. Delaroche, Phys. Rev. C **60**, 054301 (1999).

[19] W. D. Myers and W. J. Swiatecki, Nucl. Phys. **81**, 1 (1966).

[20] W. Nazarewicz, J. Dudek, R. Bengtsson, T. Bengtsson, and I. Ragnarsson, Nucl. Phys. **A435**,

397 (1985).

[21] W. Satuła, R. Wyss, and P. Magierski, Nucl. Phys. **A578**, 45 (1994).

[22] F. R. Xu, P. M. Walker, and R. Wyss, Phys. Rev. C **59**, 731 (1999).

[23] F. R. Xu, P. M. Walker, J. A. Sheikh, and R. Wyss, Phys. Lett. **B435**, 257 (1998).

[24] P. Möller and J. R. Nix, Nucl. Phys. **A536**, 20 (1992).

[25] P. Möller, J. R. Nix, W. Myers, and W. Swiatecki, Atomic Data and Nuclear Data Tables **59**, 185 (1995).

[26] F. R. Xu, W. Satuła, and R. Wyss, Nucl. Phys. **A669**, 119 (2000).

[27] H. Sakamoto and T. Kishimoto, Phys. Lett. **B245**, 321 (1990).

[28] W. Satuła and R. Wyss, Phys. Rev. C **50**, 2888 (1994).

[29] R. Wyss and W. Satuła, Phys. Lett. **B351**, 393 (1995).

[30] A. Lopez-Martens, F. Hannachi, A. Korichi, C. Schück, E. Gueorguieva, C. Vieu, B. Haas, R. Lucas, A. Astier, G. Baldsiefen, et al., Phys. Lett. **B380**, 18 (1996).

[31] K. Hauschild, L. A. Bernstein, J. A. Becker, D. E. Archer, R. W. Bauer, D. P. McNabb, J. A. Cizewski, K.-Y. Ding, W. Younes, R. Krcken, et al., Phys. Rev. C **55**, 2819 (1997).

[32] A. N. Wilson, G. D. Dracoulis, A. P. Byrne, P. M. Davidson, G. J. Lane, R. M. Clark, P. Fallon, A. Görgen, A. O. Macchiavelli, and D. Ward, Phys. Rev. Lett. **90**, 142501 (2003).

[33] A. N. Wilson, A. K. Singh, H. Hübel, P. M. Davidson, A. Görgen, D. Roßbach, A. Korichi, A. Astier, F. Azaiez, D. Bazzacco, et al., Phys. Rev. Lett. **95**, 182501 (2005).

[34] A. N. Wilson, J. Timár, J. F. Sharpey-Schafer, B. Crowell, M. P. Carpenter, R. V. F. Janssens, D. J. Blumenthal, I. Ahmad, A. Astier, F. Azaiez, et al., Phys. Rev. C **54**, 559 (1996).

[35] G. D. Dracoulis, F. G. Kondev, and P. M. Walker, Phys. Lett. **B419**, 7 (1998).

[36] A. N. Wilson, G. D. Dracoulis, P. M. Davidson, A. P. Byrne, R. M. Clark, P. Fallon, A. Görgen, G. J. Lane, A. O. Macchiavelli, and D. Ward, Nucl. Phys. **A748**, 12 (2005).

[37] U. J. van Severen, R. M. Clark, R. Krückend, H. Hübel, S. J. Asztalos, J. A. Becker, B. C. Busse, M. A. Deleplanque, R. M. Diamond, P. Fallon, et al., Phys. Lett. **B434**, 14 (1998).

[38] D. Roßbach, A. Görgen, H. Hübel, E. Mergel, G. Schönwaßer, F. Azaiez, C. Bourgeois, F. Hannachi, A. Korichi, A. Lopez-Martens, et al., Phys. Rev. C **66**, 024316 (2002).

[39] X. L. Han and C. L. Wu, At. Data Nucl. Data Tables **73**, 43 (1999).

[40] S. Leoni, G. Benzoni, A. Bracco, N. Blasi, F. Camera, C. Grassi, P. Mason, B. Million, A. Paleni, M. Pignanelli, et al., Phys. Rev. C **72**, 034307 (2005).

[41] G. Benzoni, A. Bracco, S. Leoni, N. Blasi, F. Camera, C. Grassi, B. Million, A. Paleni, M. Pignanelli, E. Vigezzi, et al., Phys. Lett. **B615**, 160 (2005).